

## University of New Hampshire University of New Hampshire Scholars' Repository

Earth Sciences Scholarship

Earth Sciences

1-30-2002

# Airborne sampling of aerosol particles: Comparison between surface sampling at Christmas Island and P-3 sampling during PEM- Tropics B

Jack E. Dibb

*University of New Hampshire*, [jack.dibb@unh.edu](mailto:jack.dibb@unh.edu)

R. Talbot

*University of New Hampshire*, [robert.talbot@unh.edu](mailto:robert.talbot@unh.edu)

Garry Seid

*University of New Hampshire - Main Campus*

C. E. Jordan

*University of New Hampshire*

Eric Scheuer

*University of New Hampshire - Main Campus*, [Eric.Scheuer@unh.edu](mailto:Eric.Scheuer@unh.edu)

*See next page for additional authors*

Follow this and additional works at: [https://scholars.unh.edu/earthsci\\_facpub](https://scholars.unh.edu/earthsci_facpub)

 Part of the [Atmospheric Sciences Commons](#)

### Recommended Citation

Dibb, J. E., R. W. Talbot, G. Seid, C. Jordan, E. Scheuer, E. Atlas, N. J. Blake, and D. R. Blake, Airborne sampling of aerosol particles: Comparison between surface sampling at Christmas Island and P-3 sampling during PEM-Tropics B, *J. Geophys. Res.*, 107, 8230, doi:10.1029/2001JD000408, 2002. [printed 108(D2), 2003]

This Article is brought to you for free and open access by the Earth Sciences at University of New Hampshire Scholars' Repository. It has been accepted for inclusion in Earth Sciences Scholarship by an authorized administrator of University of New Hampshire Scholars' Repository. For more information, please contact [nicole.hentz@unh.edu](mailto:nicole.hentz@unh.edu).

---

**Authors**

Jack E. Dobb, R. Talbot, Garry Seid, C. E. Jordan, Eric Scheuer, Elliot Atlas, Nicola J. Blake, and D R. Blake

## Airborne sampling of aerosol particles: Comparison between surface sampling at Christmas Island and P-3 sampling during PEM-Tropics B

Jack E. Dibb, Robert W. Talbot, Garry Seid, Carolyn Jordan, and Eric Scheuer

Institute for the Study of Earth, Oceans, and Space, University of New Hampshire, Durham, New Hampshire, USA

Elliot Atlas

ACD, National Center for Atmospheric Research, Boulder, Colorado, USA

Nicola J. Blake and Donald R. Blake

Chemistry Department, University of California-Irvine, Irvine, California, USA

Received 25 January 2001; revised 21 June 2001; accepted 10 July 2001; published 13 November 2002.

[1] Bulk aerosol sampling of soluble ionic compounds from the NASA Wallops Island P-3 aircraft and a tower on Christmas Island during PEM-Tropics B provides an opportunity to assess the magnitude of particle losses in the University of New Hampshire airborne bulk aerosol sampling system. We find that most aerosol-associated ions decrease strongly with height above the sea surface, making direct comparisons between mixing ratios at 30 m on the tower and the lowest flight level of the P-3 (150 m) open to interpretation.

Theoretical considerations suggest that vertical gradients of sea-salt aerosol particles should show exponential decreases with height. Observed gradients of  $\text{Na}^+$  and  $\text{Mg}^{2+}$ , combining the tower observations with P-3 samples collected below 1 km, are well described by exponential decreases ( $r$  values of 0.88 and 0.87, respectively), though the curve fit underestimates average mixing ratios at the surface by 25%. Cascade impactor samples collected on the tower show that >99% of the  $\text{Na}^+$  and  $\text{Mg}^{2+}$  mass is on supermicron particles, 65% is in the 1–6 micron range, and just 20% resides on particles with diameters larger than 9 microns. These results indicate that our airborne aerosol sampling probes must be passing particles up to at least 6 microns with high efficiency. We also observed that nss  $\text{SO}_4^{2-}$  and  $\text{NH}_4^+$ , which are dominantly on accumulation mode particles, tended to decrease between 150 and 1000 m, but they were often considerably higher at the lowest P-3 sampling altitudes than at the tower. This finding is presently not well understood. *INDEX TERMS:* 0305

Atmospheric Composition and Structure: Aerosols and particles (0345, 4801); 0365 Atmospheric Composition and Structure: Troposphere—composition and chemistry; 0394 Atmospheric Composition and Structure: Instruments and techniques; 9355 Information Related to Geographic Region: Pacific Ocean; *KEYWORDS:* airborne aerosol sampling, inlet passing efficiency, tropical Pacific, PEM Tropics B

**Citation:** Dibb, J. E., R. W. Talbot, G. Seid, C. Jordan, E. Scheuer, E. Atlas, N. J. Blake, and D. R. Blake, Airborne sampling of aerosol particles: Comparison between surface sampling at Christmas Island and P-3 sampling during PEM-Tropics B, *J. Geophys. Res.*, 107, 8230, doi:10.1029/2001JD000408, 2002. [printed 108(D2), 2003]

### 1. Introduction

[2] PEM-Tropics B, the fourth in the NASA Global Tropospheric Experiment Pacific Exploratory Mission series, was conducted in March–April 1999. Like PEM-Tropics A, the B campaign deployed the Wallops Island P-3 and the Dryden DC-8 to the central and western south Pacific. Differences in the capabilities of the two platform aircraft, and in the instrumentation on board, lead to different primary objectives and flight profiles [Raper *et al.*, 2001; Davis *et al.*, 2002a; Jacob *et al.*, in press]. The principal objectives of the P-3 component were to improve

understanding of the sulfur cycle and the factors controlling OH in the tropical oceanic atmosphere.

[3] We measured the aerosol-associated end products of the sulfur cycle, non-sea-salt sulfate (nss- $\text{SO}_4^{2-}$ ) and methylsulfonate ( $\text{MS}^-$ ) collected on filters from the P-3. Davis *et al.* [2002b] use measurements from the P-3 to assess whether the Georgia Tech 0-dimensional, or point, model of sulfur cycling in the marine boundary layer is consistent with the observations made during PEM-Tropics B. In general, the model predicts significantly more nss  $\text{SO}_4^{2-}$  than we measured. Davis *et al.* [2002b] recognize that the chemistry in the model may not be complete and that the lifetime of nss  $\text{SO}_4^{2-}$  in the marine boundary is not very well constrained, but also suggest that part of the discrepancy

**Table 1.** Summary of Selected Aerosol-Associated Ionic Species Collected at 30 m asl on the Christmas Island Tower on 16–22 March 1999<sup>a,b</sup>

	Na <sup>+</sup>	Mg <sup>2+</sup>	NO <sub>3</sub> <sup>-</sup>	Total SO <sub>4</sub> <sup>2-</sup>	MS <sup>-</sup>	nss <sup>c</sup> SO <sub>4</sub> <sup>2-</sup>	NH <sub>4</sub> <sup>+</sup>
mean	4677	509	22	416	12	141	256
s.e. <sup>d</sup>	438	49	2	31	1	8	16
median	4193	430	22	378	10	149	252
range	2086–10,835	220–1213	3–43	246–879	5–25	71–233	113–401

<sup>a</sup>On most days, two or three 3- to 4-h-long samples were collected during daylight hours. On 21 March, two cascade impactor samples were collected for sequential 6-h intervals, and on 22 March, 11 nominally 1-h-long samples were collected between 0640 and 1840 h local time.

<sup>b</sup>Mixing ratios are reported in parts per trillion by volume (pptv).

<sup>c</sup>Sea-salt SO<sub>4</sub><sup>2-</sup> was estimated from Mg<sup>2+</sup>.

<sup>d</sup>s.e. = standard error of the mean.

could be due to the difficulty of sampling aerosols from aircraft. They point out that observed mixing ratios could be biased low by losses in the sampling probe upstream of the filter. *Chin et al.* [2000] likewise suggest undersampling of aerosols as a partial explanation for the tendency of the global chemical transport model (CTM) GOCART to estimate mixing ratios twice as high as our measurements of SO<sub>4</sub><sup>2-</sup> over the Pacific ocean during the GTE PEM West A and B and PEM-Tropics A campaigns. On the other hand, *Xiao et al.* [1997] compared predictions of SO<sub>2</sub>, SO<sub>4</sub><sup>2-</sup> and dust from the regional-scale CTM STEM-II to selected PEM West B flights and found encouraging agreement.

[4] Several modeling groups have recently highlighted the importance of correctly parameterizing wet and dry removal processes in CTMs, and focus on the <sup>222</sup>Rn–<sup>210</sup>Pb system as a nearly ideal test case due to the lack of any chemical impacts on the distributions of these tracers in the atmosphere. *Guelle et al.* [1998] point out that several parameterizations of precipitation scavenging can reproduce observed spatial patterns in the deposition and surface concentrations of <sup>210</sup>Pb reasonably well, but that they predict radically different distributions in the vertical. Since long-range transport is so strongly controlled by vertical distribution, this aspect of CTMs must be depicted correctly. *Giannakopoulos et al.* [1999] conducted a similar test of parameterizations of wet scavenging, and also dry deposition, within a different CTM and followed the lead of *Guelle et al.* [1998] by highlighting the value of the PEM West <sup>210</sup>Pb data set (that we generated with an aerosol sampling probe identical to the one used for SO<sub>4</sub><sup>2-</sup>) as a means to compare the effects of the various formulations of the removal processes. In a follow up paper, *Giannakopoulos et al.* [2000] were able to attribute disagreement between modeled and observed PAN to their chemistry formulation since good simulation of <sup>210</sup>Pb made them confident that transport/precipitation was well simulated.

[5] In order to use airborne observations of aerosol-associated compounds as a strong challenge to present and future CTMs, we must establish the magnitude of any artifacts introduced in collection of such samples. *Huebert et al.* [1990] present clear evidence that inlet losses can be very substantial, particularly for sampling probes that use knife edge nozzles. Unfortunately, *Huebert et al.* [1990] implied that the results of the PASIN study were representative of all aerosol sampling probes. *Porter et al.* [1992] provided evidence that the situation is not so bleak, but reinforced the importance of taking all possible steps to reduce aerosol losses in sampling probes, and to characterize the magnitude

of such losses as well as possible for each specific probe used for aerosol collection. *Baumgardner et al.* [1991] outlined the specific problems with sampling particles from aircraft, and recommended means to reduce them.

[6] Here we compare aerosol-associated soluble ion mixing ratios determined from the P-3 to tower-based measurements made on Christmas Island during the PEM-Tropics B mission. Our intent is to constrain the magnitude of particle losses in the airborne sampling probe, assuming that any sampling bias for the stationary, inlet-free, system on the tower will be insignificant compared to the magnitude of discrepancies between model predictions and our observations. The geochemical implications of our aerosol-associated sulfur compound mixing ratios are discussed in the context of the full PEM-Tropics B data set by *Davis et al.* [2002b], *Nowack et al.* [2002] and *Oncley et al.* [2002].

## 2. Methods

### 2.1. Sampling

[7] PEM-Tropics B was the first time that the UNH aerosol sampling system has been flown on the NASA P-3. Our aerosol sampling system was modeled on the one we have flown on all of our deployments on the DC-8 [*Dibb et al.*, 1996, 1997, 1998, 1999, 2000], employing curved leading edge (CLE) nozzles centered in a shroud that extends 20 cm forward of the nozzle. This design has evolved through the course of RWT's participation in GTE campaigns. During the ABLE 2A and 2B deployments about 20 paired samples were collected through dual probes which differed only in that one probe used a CLE nozzle while the second used a sharp edged nozzle (like those tested in the PASIN study [*Huebert et al.*, 1990]). Concentrations of soluble ions predominantly found on supermicron particles were invariably higher in the CLE samples by factors of 1.5–3.0 (averaging roughly twofold higher). Further testing of the CLE probe during ABLE 2 showed that 75–85% of C<sub>2</sub>O<sub>4</sub><sup>2-</sup> (a tracer of combustion which is dominantly found on coarse particles) which entered the nozzle was collected on the filter, with the balance lost by deposition in the nozzle (5–10%) and in the inlet tubing (10–15%). For the ABLE 3A campaign the shroud around the nozzle was added in order to straighten streamlines and allow for more nearly isoaxial sampling as the aircraft pitch angle varied during flight. Eight pairs of samples comparing CLE probes, with one inside a shroud and the other not shrouded, were collected during ABLE 3A. Concentrations of coarse-particle-associated ions like Na<sup>+</sup> and NO<sub>3</sub><sup>-</sup> were enhanced by

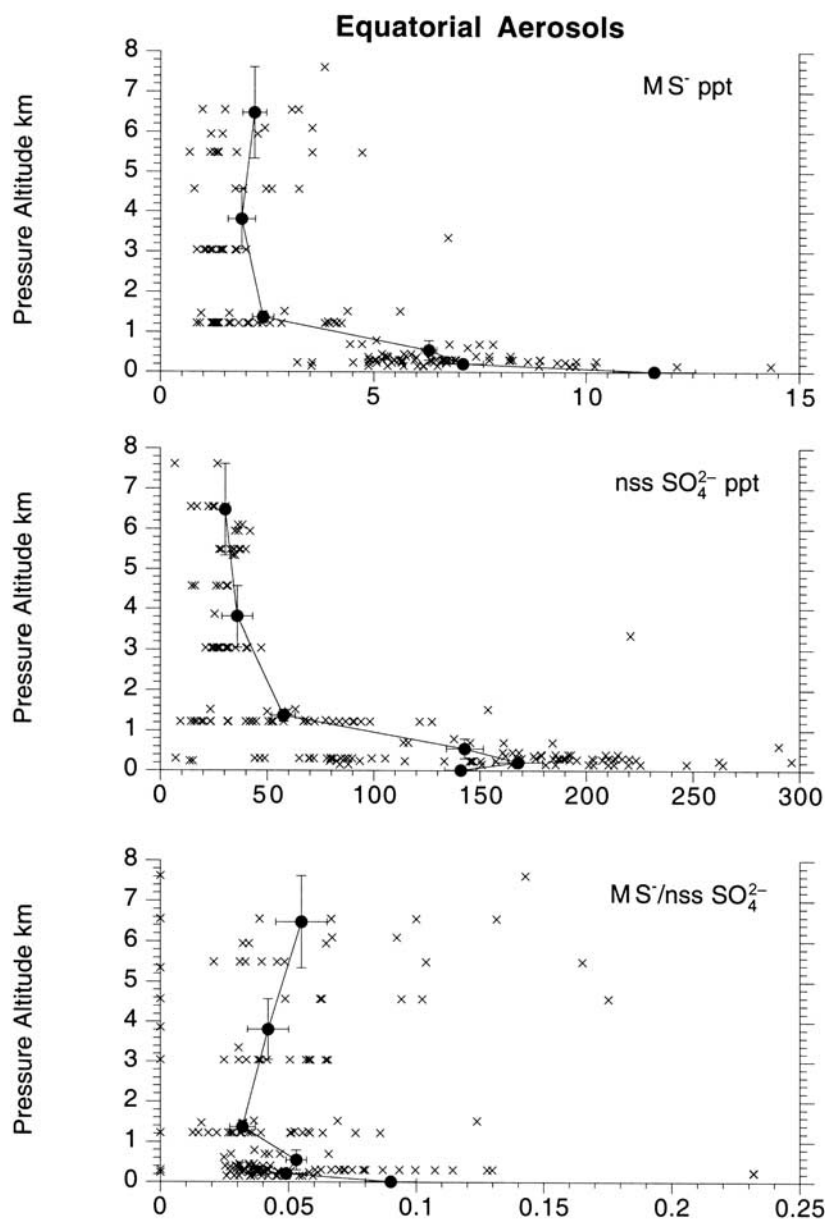


**Figure 1.** Mixing ratios of MS<sup>-</sup> and nss SO<sub>4</sub><sup>2-</sup> measured from the P-3 during PEM-Tropics B Flights 5–12 in the vicinity of Christmas Island. The lower panel displays the ppt/ppt (molar) ratio. All P-3 samples above detection limit are shown as small x's. The dots are plotted at the mean mixing ratios in 5 altitude bins, with the 6th (lowest) dot representing the means for all samples collected at 30 m from the Christmas Island tower. For the P-3 altitude bins the vertical error bars cover the altitude range included in each bin and the horizontal error bars show the standard error of the mean.

30–50% in the samples collected with the shrouded probe. Fine-particle-associated SO<sub>4</sub><sup>2-</sup> and NH<sub>4</sub><sup>+</sup> concentrations were also enhanced by the shroud, but only rarely by so much as 10%. As a result of this series of tests, when GTE moved to the NASA Ames DC-8 (now based at NASA Dryden) for the Pacific Exploratory Mission series, RWT designed an aerosol sampling probe with a shrouded CLE nozzle. The DC-8 probes (and also those for the P-3) use stainless steel tubes with diameters twice those employed on earlier ABLE campaigns on the Electra, and increased the radius of the single bend required to bring air inside of the airplane as much as possible. These changes were

implemented to reduce losses of particles by deposition in the tubing downstream of the nozzles. The size of these probes, and details of their installation, have precluded collection of quantitative rinses to assess the magnitude of any particle losses that may still be occurring within the inlet tubing.

[8] The CLE nozzles deployed on the P-3 for PEM-Tropics B expand from the initial diameter of 0.5 cm at 7° to meet the 5 cm OD seamless stainless steel inlet which bends 30° with a radius of curvature of 43 cm to penetrate the aircraft window plate. Immediately inside the fuselage a Delrin ball valve is followed by a Delrin diffuser (again 7°)

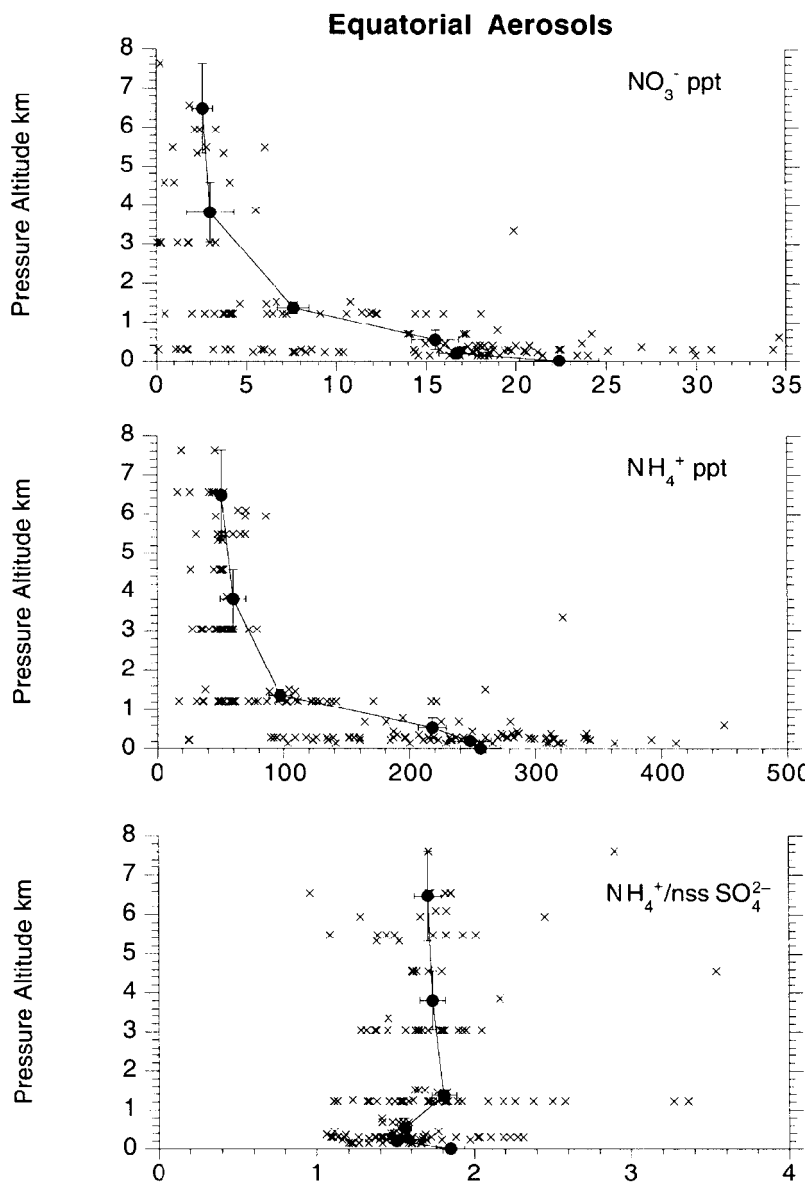


Figure 2. As in Figure 1, but for  $\text{NO}_3^-$ ,  $\text{NH}_4^+$  and the  $\text{NH}_4^+/\text{nss SO}_4^{2-}$  ratio.

that terminates in a Delrin holder for the 9 cm diameter Teflon filter. Downstream of the filter the system consists of another valve (to isolate the filter holder in order to change filters and also allow flow adjustment to maintain isokinetic sampling), a mass flowmeter to measure sample flow rates and volume, and a venturi pump to provide vacuum. Sampling flow rates were manually adjusted to be isokinetic within 10% along each level flight leg.

[9] We have used Gelman Zefluor filters in all of our recent airborne aerosol sampling campaigns. New lots of Zefluor filters purchased for PEM-Tropics B contained unacceptably high and variable blank values for several ions. After extensive testing of available replacement filter media we selected 9 cm diameter 2 micron Millipore Fluoropore Teflon filters for PEM-Tropics B.

[10] A total of 326 aerosol samples were collected on level flight legs during the 17 flights of this mission. The complete

data set is archived at, and available from, the GTE project office at NASA Langley. Our focus in this paper will be restricted to the 8 flights that centered on Christmas Island (P-3 Flights 5–12). These flights all targeted the S cycle in the equatorial Pacific boundary layer [Davis *et al.*, 2002a; Raper *et al.*, 2001] and yielded 172 filter samples for quantitation of water soluble aerosol-associated ions.

[11] While the P-3 was based on Christmas Island we also collected aerosol samples from a tower on the island, about 100 m from the shoreline, between 16 and 22 March 1999. All samples were collected from a height 30 m asl with an open-faced, downward pointing filter holder. During the first five days two or three 3- to 4-h long bulk samples were collected each day during daylight hours. Two 6-h long cascade impactors were exposed sequentially on 21 March, and eleven 1-h long bulk samples were collected between 0640 and 1840 h local time on 22 March. All of these

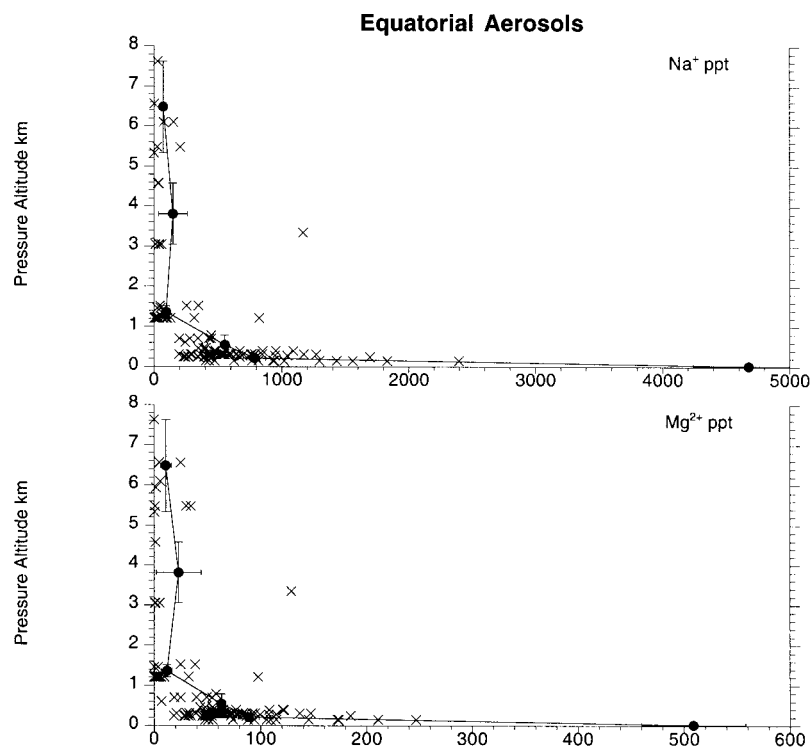


Figure 3. As in Figure 1, but for  $\text{Na}^+$  and  $\text{Mg}^{2+}$ .

samples were collected on the same Fluoropore media as was used on the P-3.

## 2.2. Analysis

[12] Filter handling after airborne sample collection followed the procedures described by *Dibb et al.* [1999, 2000], including purging the sample bags with zero air to exclude cabin air. Tower samples were sealed in bags for transport between the tower and lab and then immediately extracted. All samples were analyzed in a field laboratory set up on Christmas Island (and then in Tahiti) within 1–2 days of collection. Inorganic anions, cations, and methylsulfonate ( $\text{MS}^-$ ) were quantified in three separate ion chromatographic runs.

[13] Variability in the mass of soluble ions contributed by unexposed filters represents a major portion of the uncertainty in calculated mixing ratios, especially for lightly loaded samples. Our change from Zefluor to Fluoropore filters resulted in significantly lower, and more stable, blank values which allowed us to shorten sample times. We generated 53 blanks during the P-3 portion of PEM-Tropics B which yielded mean (standard deviation) concentrations of 16.4 (6.1), 2.2 (1.5), 0.9 (0.8), 0.7 (0.4), 0.7 (0.5) nmol filter<sup>-1</sup> of  $\text{Na}^+$ ,  $\text{NH}_4^+$ ,  $\text{Mg}^{2+}$ ,  $\text{NO}_3^-$ , and  $\text{SO}_4^-$ , respectively. Methylsulfonate could not be detected on any of the blanks. For all species except  $\text{Mg}^{2+}$  these means, and particularly the variability, are > twofold lower than we obtained for Zefluor filters during PEM-Tropics A [see *Dibb et al.*, 1999].

[14] During Flights 5–12 our mean (median) filter exposure period was 15.9 (14) minutes, corresponding to mean (median) sample volumes of 2.83 (2.65) standard cubic meters (scm). Sampling times were shorter in the boundary

layer (mean 13.4 min below 1 km versus 18.4 min at higher altitudes), though the higher mass flow rates possible at lower altitudes resulted in similar sample volumes between the boundary layer and above (2.85 scm below 1 km, 2.81 scm above). For a sample with mean volume, the uncertainty in the blanks translates to uncertainty in mixing ratios of 49, 12, 6, 3, and 4 ppt for  $\text{Na}^+$ ,  $\text{NH}_4^+$ ,  $\text{Mg}^{2+}$ ,  $\text{NO}_3^-$ , and  $\text{SO}_4^-$ , respectively. The much larger sample volumes for the bulk samples collected on the Christmas Island tower means that uncertainty in the blank contributed less to uncertainty in mixing ratios.

## 3. Results

[15] Mixing ratios of selected aerosol-associated soluble ions collected on the Christmas Island tower are summarized in Table 1. The most direct comparison to previous results can be made to the July and August 1994, sampling campaign reported by *Huebert et al.* [1996]. Unfortunately, these authors only provide results for  $\text{MS}^-$  and nss  $\text{SO}_4^{2-}$ . Our median  $\text{MS}^-$  mixing ratio (10 pptv) is identical to that in the earlier study, though we encountered both higher and lower extremes than the 7–19 pptv range observed during 10 days of intensive sampling in the *Huebert et al.* [1996] experiment. In contrast, median nss  $\text{SO}_4^{2-}$  during our sampling was only 2/3 that observed in 1994, in fact, our maximum mixing ratio (233 ppt) (Table 1) barely exceeded the median (221 ppt) found in 1994.

[16] Aerosols and gases have been collected in the marine boundary layer of the equatorial Pacific, sometimes quite near to Christmas Island, on a number of cruises [e.g., *Bates et al.*, 1989, 1992; *Quinn et al.*, 1990; *Clarke and Porter*,

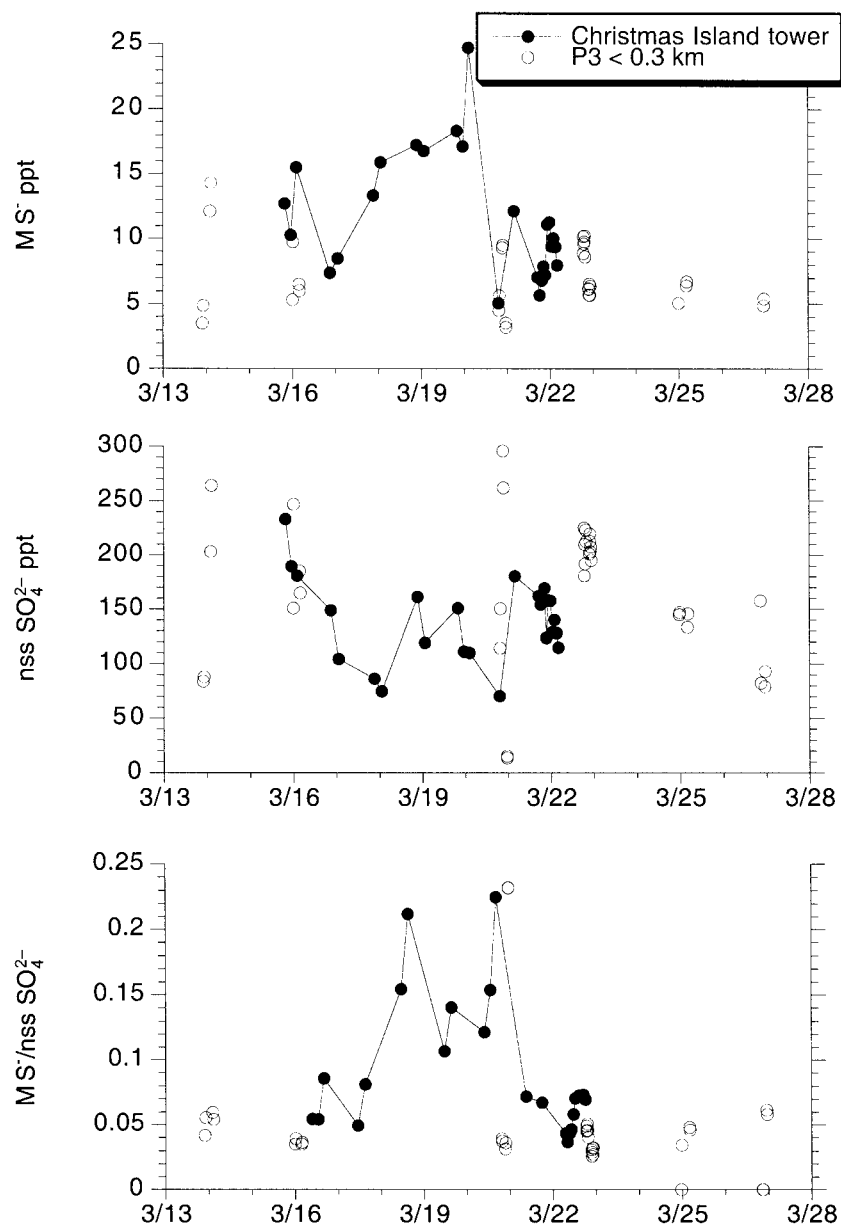


**Figure 4.** Mixing ratios of  $\text{MS}^-$  and  $\text{nss SO}_4^{2-}$  measured at 30 m asl at the Christmas Island tower and from the P-3 at altitudes between 150 and 270 m. The lower panel displays the ppt/ppt (molar) ratio. Sampling at the tower was not continuous through the nighttime hours (see Table 1). All data are plotted against Greenwich Meridian time, local time at Christmas Island is 14 h ahead.

1993]. However, these investigators employed size selective inlets to exclude supermicron particles, or used thermal techniques to infer particle composition, hence the results are not readily compared to our bulk samples. *Savoie et al.* [1994] reported average mixing ratios of 5000, 41, 5, and 87 ppt for  $\text{Na}^+$ ,  $\text{NO}_3^-$ ,  $\text{MS}^-$  and  $\text{nss SO}_4^{2-}$ , respectively, for bulk aerosol samples collected 20 m asl at American Samoa between 1983 and 1992. We recognize that Samoa is more than 10 degrees west, and nearly 15 degrees south, of Christmas Island hence may generally be exposed to different air masses. Therefore, it may be largely fortuitous that our mean mixing ratios of  $\text{NO}_3^-$  and the particulate S species are within a factor of 2 of those measured at Samoa ( $\text{NO}_3^-$

higher at Samoa and the S species higher at Christmas) (Table 1). On the other hand, sea-salt mixing ratios should be largely driven by wind speeds rather than proximity to specific source regions (either oceanic or continental). The fact that our mean  $\text{Na}^+$  mixing ratio is only 7% lower than the long-term mean at Samoa provides some reassurance that our short experiment at Christmas Island provides a representative impression of the tropical Pacific marine boundary layer.

[17] Over the course of 8 flights (covering a two-week interval) the P-3 encountered considerable variability in the mixing ratios of all aerosol species in all altitude bins. However, the mean mixing ratios of  $\text{nss SO}_4^{2-}$  and  $\text{NH}_4^+$  in



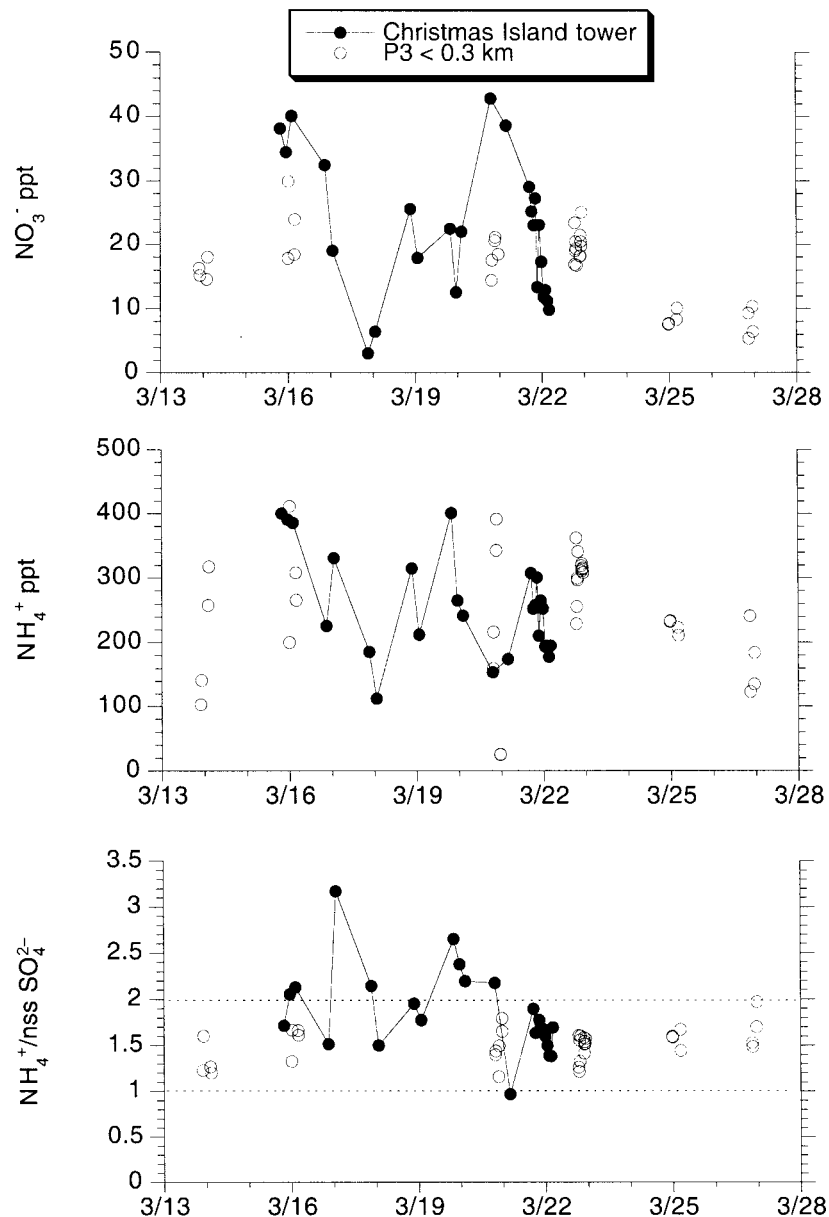


**Figure 5.** As in Figure 4, but for  $\text{NO}_3^-$ ,  $\text{NH}_4^+$  and the  $\text{NH}_4^+/\text{nss SO}_4^{2-}$  ratio.

the 0.15–0.3 and 0.3–0.8 km altitude bins were within 16% of the means measured at 30 m on the tower (Figures 1 and 2). It should be noted that the mean nss  $\text{SO}_4^{2-}$  mixing ratio was higher in the lowest P-3 altitude bin than on the tower, though the large range in both data sets makes the significance of this point difficult to assess. This contrasts the cases for  $\text{NO}_3^-$  and  $\text{MS}^-$ , where the mean mixing ratios at the tower exceeded those in the P-3 boundary layer samples by 30–50% (Figures 1 and 2), and for  $\text{Na}^+$  and  $\text{Mg}^{2+}$  with mean mixing ratios roughly sixfold higher at 30 meters on the tower than in P-3 samples collected between 150 and 300 meters (Figure 3). Non-sea-salt  $\text{SO}_4^{2-}$  and  $\text{NH}_4^+$  are generally felt to be predominantly on submicron particles,  $\text{NO}_3^-$  and  $\text{MS}^-$  can have appreciable mass in supermicron fractions, while  $\text{Na}^+$  and  $\text{Mg}^{2+}$  are dominantly associated with the supermicron particles. These observations could indicate

that our sampling system on the P-3 is efficiently passing submicron particles, but is severely biased against supermicron particles. On the other hand, it has long been known that sea-salt mass concentrations (which are dominated by  $\text{Na}^+$  and  $\text{Cl}^-$ ) decrease with height above the ocean [Blanchard and Woodcock, 1980], thus the  $\text{Na}^+$  and  $\text{Mg}^{2+}$  gradients we observed may be real. Of course, it is also possible that our results reflect real vertical gradients exaggerated by losses of large particles in our sampling inlet. The combined tower and P-3 data sets constitute a unique field intercomparison that may help to define the magnitude of particle losses in our P-3 aerosol sampling probes as a function of particle size. We expect that the transmission efficiency of the probes we fly on the DC-8 should be similar, yet acknowledge at the outset that the comparisons made below are not definitive even for the P-3 system and further

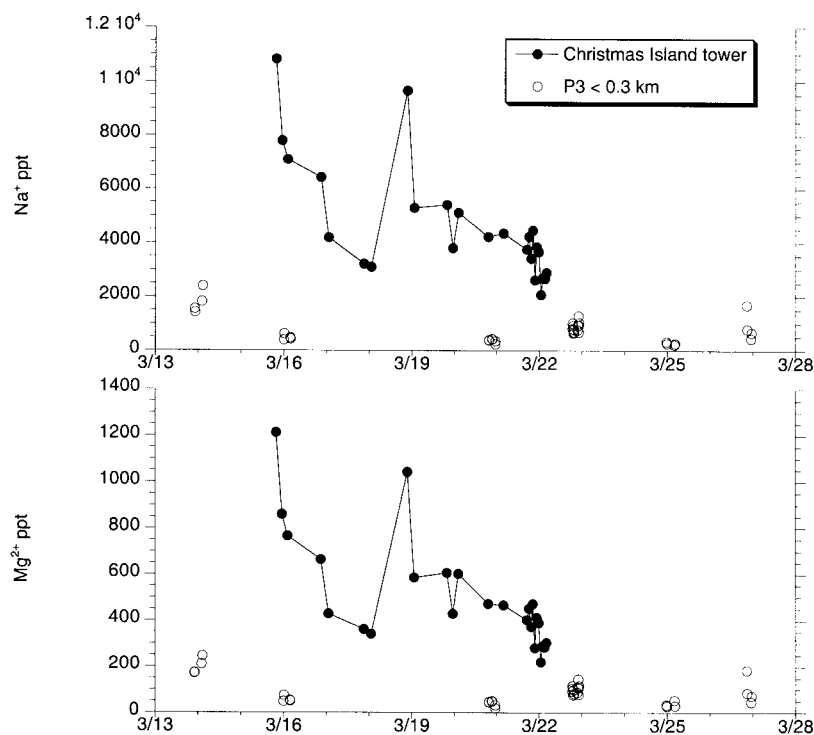


Figure 6. As in Figure 4, but for  $\text{Na}^+$  and  $\text{Mg}^{2+}$ .

controlled tests of all airborne aerosol sampling probes are still needed.

#### 4. Discussion

[18] More than half of the sampling days at the tower occurred when the P-3 remained on the ground or conducted flights that did not include any sampling below 300 meters (Figures 4–6). We expected that the equatorial Pacific boundary layer would be quite homogeneous spatially, translating into small temporal variability at any fixed location as the steady winds advected similar air masses day to day [Bandy *et al.*, 1996; Huebert *et al.*, 1996] (D. Davis, personal communication, March 1999). During the PEM-Tropics B deployment rain events and convective mixing of free tropospheric air into the boundary layer around Christmas Island were much more frequent than expected. As a result, the time series at the Christmas Island tower were characterized by 3- to fivefold variations in mixing ratios of aerosol-associated species from one day to the next as particle-depleted air masses (scavenged within the boundary layer by rain or mixed downward from the free troposphere) alternated with more aged boundary layer air (Figures 4–6). Particularly large variations were observed 16–20 March, with nss  $\text{SO}_4^{2-}$ ,  $\text{NO}_3^-$ ,  $\text{NH}_4^+$ ,  $\text{Na}^+$  and  $\text{Mg}^{2+}$  mixing ratios all approaching campaign minima early in the interval but rebounding sharply through the 19th and 20th. In contrast,  $\text{MS}^-$  steadily increased to the highest levels we observed at the tower. Throughout this interval we have no low-level samples from the P-3. Flights 7 and 8 were flown 17–18 March, but these were

the only flights in the Christmas Island portion of the mission that included no sampling below 300 meters. The demonstrated short-term variability at the tower, and the timing of extremes in mixing ratios that were inadvertently missed in the low-level P-3 sampling, suggests that comparing the 7-day averages from the P-3 to the largely noncoincident 7-day averages at the tower (as was done in Figures 1–3), may be misleading. Fortunately, the final day of filter sampling (with the 1-h collection interval) at the tower was conducted the day before P-3 Flight 10 where most of the 10-h flight was spent in the boundary layer and buffer layer. The final sample at the tower was collected just 10 h before the P-3 took off (Figures 4–6). Focusing just on these two days may provide a more realistic comparison.

[19] Flight 10 of the P-3 was a sunrise flight designed to constrain DMS flux, and then to follow the photochemical transformation of DMS through the morning and early afternoon [Raper *et al.*, 2001; Davis *et al.*, 2002a]. The flight plan called for a series of Lagrangian circles in the boundary and buffer layers, interrupted by just a few brief forays into the free troposphere (in an attempt to cool the airplane). For the present purposes we are particularly interested in the steep mixing ratio gradients of aerosol-associated species (Figures 7 and 8) (as well as many trace gases derived from the surface ocean).

[20] Our measurements of sea-salt derived ions appear to provide important insight into the performance of the aerosol sampling system we flew on the P-3. Mass-size distributions obtained from the two cascade impactor samples collected on the tower 21 March (Christmas Island

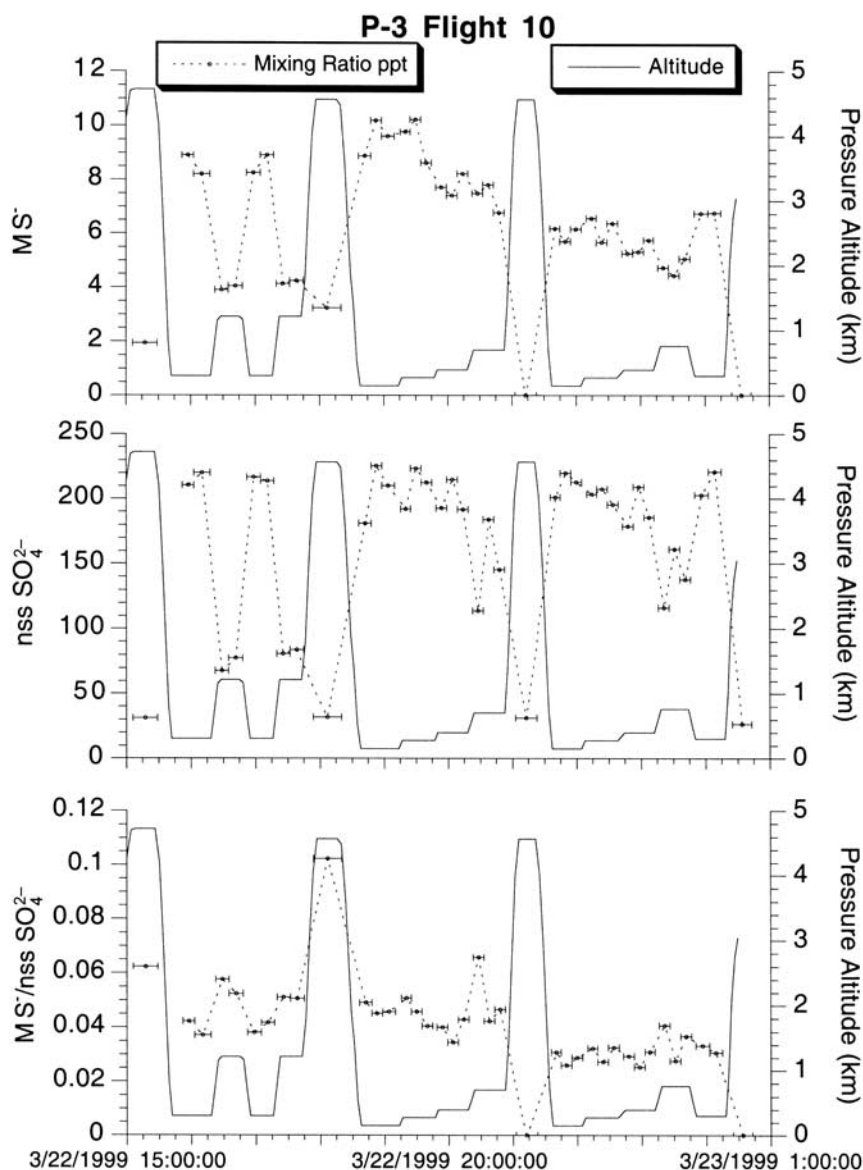


**Figure 7.** Mixing ratios  $MS^-$  and  $nss\ SO_4^{2-}$  measured from the P-3 during PEM-Tropics B Flight 10. The solid line shows the flight altitude of the aircraft. Error bars on the mixing ratio data points depict the interval over which each filter was exposed (on the order of 10 min or less in the boundary and buffer layers). The lower panel displays the ppt/ppt (molar) ratio. Times are given in UT, local time is 14 h ahead (2200 UT is noon Christmas Island time on the following day).

time) confirm the expectation that most sea-salt aerosol mass is associated with supermicron particles (>99% of  $Na^+$  and  $Mg^{2+}$  found in the supermicron fraction, and 20% on particles with diameters >9 microns (Table 2)). If our sampling system has poor passing efficiency for large particles, it should be most apparent for species that are dominantly derived from sea-salt.

[21] Mixing ratios of  $Na^+$  and  $Mg^{2+}$  in all P-3 Flight 10 samples within the bottom kilometer of the atmosphere decreased rapidly with height. At the lowest aircraft sampling altitude the mixing ratios were 2- to fivefold lower than the range measured at 30 m on the tower less than a day earlier (Figure 9), similar to the sixfold higher

overall mean mixing ratios at the tower shown in Figure 3. However, these steep gradients are consistent with theory and limited experimental data that suggest that sea-salt derived particles should decrease with height above the ocean source. *Blanchard and Woodcock* [1980] suggested that the average decrease could be described by a power law relation, incorporating wind speed, while *Neele et al.* [1998] indicate that the steady state profile should decrease exponentially with height. Fitting exponential curves through the combined  $Na^+$  and  $Mg^{2+}$  data from Flight 10 and the tower (Figure 9) yields estimated surface mixing ratios that are 75% of the means measured at the tower (but are within one standard deviation of the tower

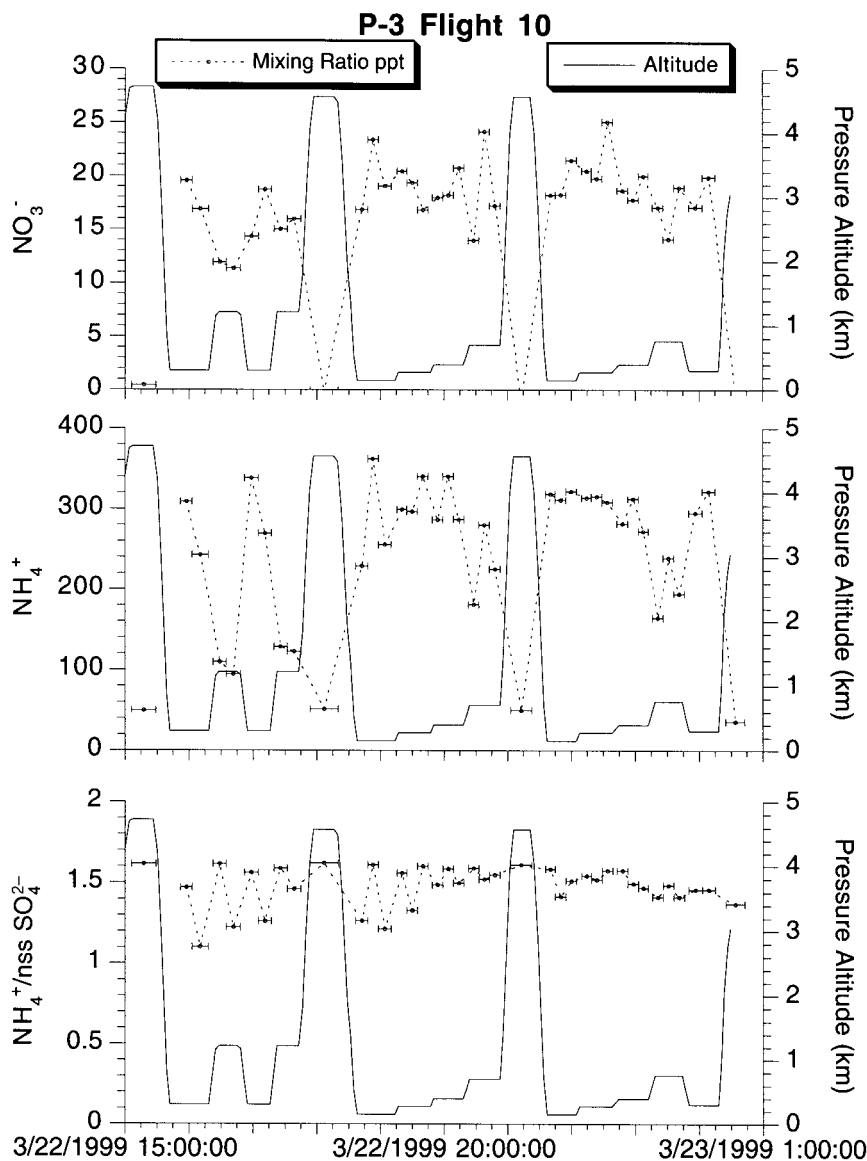


Figure 8. As in Figure 5, but for  $\text{NO}_3^-$ ,  $\text{NH}_4^+$  and the  $\text{NH}_4^+/\text{nss SO}_4^{2-}$  ratio.

means for both  $\text{Na}^+$  and  $\text{Mg}^{2+}$ ). The 95% uncertainty estimates of the curve fit intercepts in Figure 9 range from 65 to 85% of the measured tower means. It is likely that the surf zone on the shore of Christmas Island generates more sea-salt aerosols than the processes of wave breaking and bubble bursting operating in the open ocean, such that we might expect a small enhancement of sea-salt at 30 m at the tower relative to the P-3 sampling area [Blanchard and Woodcock, 1980]. One could argue that higher sea-salt mixing ratios at 30 m on the tower than would be consistent with the P-3 observations, while barely statistically evident, provide evidence of enhancement due to the island and breaking surf. However, if we assume that the comparison between surface concentrations estimated from the curve fit and the tower measurements indicates that the aircraft is only sampling 75% of the sea-salt particles, the mass size distributions at Christmas Island (Table 2) suggest that our system is efficiently sampling all particles <6 microns and must be passing a significant fraction of

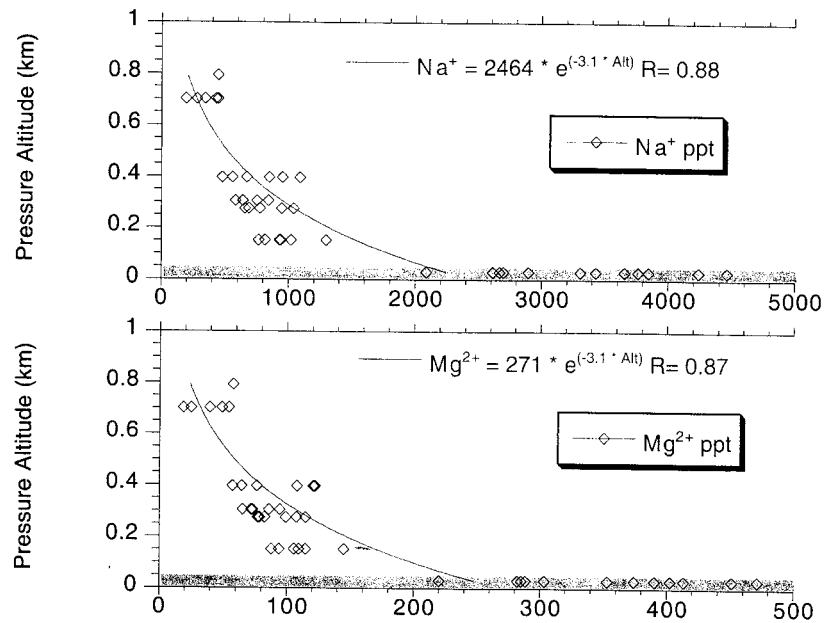
the particles approaching 9 microns. In fact, this analysis is probably overly stringent for yet another reason, since the steepness of vertical gradients of particles derived from the ocean surface is a strong function of particle

Table 2. Cumulative Mass<sup>a</sup> of Soluble Ions as a Function of Particle Diameter<sup>b</sup>

Cut Size, microns	$\text{Na}^+$	$\text{Mg}^{2+}$	$\text{NO}_3^-$	Total $\text{SO}_4^{2-}$	$\text{MS}^-$	nss $\text{SO}_4^{2-}$	$\text{NH}_4^+$
<1.1	0.9	0.5	2.9	30.9	57.3	73.5	75.3
<2.1	10.9	10.5	18.7	39.7	83.0	80.4	78.2
<3.3	30.3	29.2	47.6	53.3	98.5	86.9	82.8
<4.7	55.6	54.3	75.3	70.2	98.5	92.3	87.5
<5.8	66.0	64.9	85.2	77.3	100.0	94.5	90.6
<9.0	80.6	80.3	93.4	87.0		96.3	93.8
<10.0	86.5	86.2	96.6	90.9		97.4	96.5
<25.0	100.0	100.0	100.0	100.0		100.0	100.0

<sup>a</sup> Cumulative mass is expressed in %.

<sup>b</sup> Two cascade impactor samples were collected on the Christmas Island tower on 21 March.



**Figure 9.** Vertical profiles of  $\text{Na}^+$  and  $\text{Mg}^{2+}$  in the lowest km of the atmosphere during P-3 Flight 10. Mixing ratios at the Christmas Island tower 10–20 h earlier on the previous day (1-h sample interval) are plotted within the grey bar. The curves are least squares best fit exponentials that include both the P-3 and tower data. For  $\text{Na}^+$  the 95% confidence interval about the exponential term ranges from  $-2.8$  to  $-3.4$  and the same confidence interval about the estimated surface mixing ratio encompasses 2227–2726 ppt. For  $\text{Mg}^{2+}$  the uncertainties in the curve fit are  $-2.8$  to  $-3.3$  for the exponential term and 245–300 ppt at the surface.

size, increasing rapidly with size [Blanchard and Woodcock, 1980; Neele et al., 1998].

[22] It is clear that sea-salt is distributed across a range of particle sizes (Table 2) and this distribution presumably shifts to smaller sizes with increasing altitude as the abundance of large particles decreases most rapidly. As a result, we would not expect a single exponential profile to describe the vertical distribution of bulk sea-salt. Rather, the distribution should reflect the sum of a family of curves. Figure 10 presents several hypothetical  $\text{Na}^+$  gradients as examples. In the upper panel the thin dotted curve depicts the slow decrease of fine particles, with an exponential term  $= -0.7$ . For this fraction we have assumed that the surface mixing ratio was 330 ppt corresponding to 10% of the mean  $\text{Na}^+$  mixing ratio at the tower, hence reflecting sea-salt aerosols with diameters  $<2$  microns (Table 2). The other three curves all assume surface mixing ratios of 2970 ppt (90% of the mean  $\text{Na}^+$  mixing ratio at the tower) which then decrease with height at arbitrary exponential rates (all of the rates are faster than the best fit exponent of  $-3.1$  (Figure 9) but we have no basis for choosing any specific values other than as illustrative). In the lower panel the three labeled curves show the sum of the presumed fine fraction gradient plus each of the hypothetical profiles for larger particles, superimposed on the measured bulk  $\text{Na}^+$  mixing ratios. All of these curves come closer to capturing the very high mixing ratios at the tower, and also the magnitude of the decrease between 30 m and the lowest

P-3 sampling altitudes, than the best fit “pure” exponential decrease which is reproduced as the heavy dashed curve (Figure 10).

[23] We hypothesize that the vertical profile of sea-salt aerosols in the marine boundary layer should be described by the sum of a wide range of exponential curves, with significant mass in the largest particle sizes rarely reaching heights above wave top, let alone the 30 m level of the tower or the 150 m minimum operational altitude of the P-3. However, we are not aware of any published data on the vertical evolution of mass-size distributions of particles above the ocean that cover the altitude and particle diameter ranges of interest. As a result, we interpret the disagreement between our measured  $\text{Na}^+$  and  $\text{Mg}^{2+}$  profiles and the single “best fit” exponential curve (Figure 9) as a clear indication that our P-3 filter samples are capturing proportionately less “very large” ( $>9$  micron) sea-salt particles than are the bulk samples collected on the tower. We suspect this is largely due to the fact that there simply are very few of these giant particles present 150 m and higher above the ocean, but must acknowledge that it is impossible to rule out the possibility that we can not sample any giant particles that might be present through our airborne sampling system.

[24] The foregoing analysis of sea-salt vertical distributions forms the basis for our belief that our airborne aerosol system passes a dominant fraction of supermicron particles up to at least 6, and perhaps nearly 10 microns. Examining the distributions of other aerosol-associated species that are

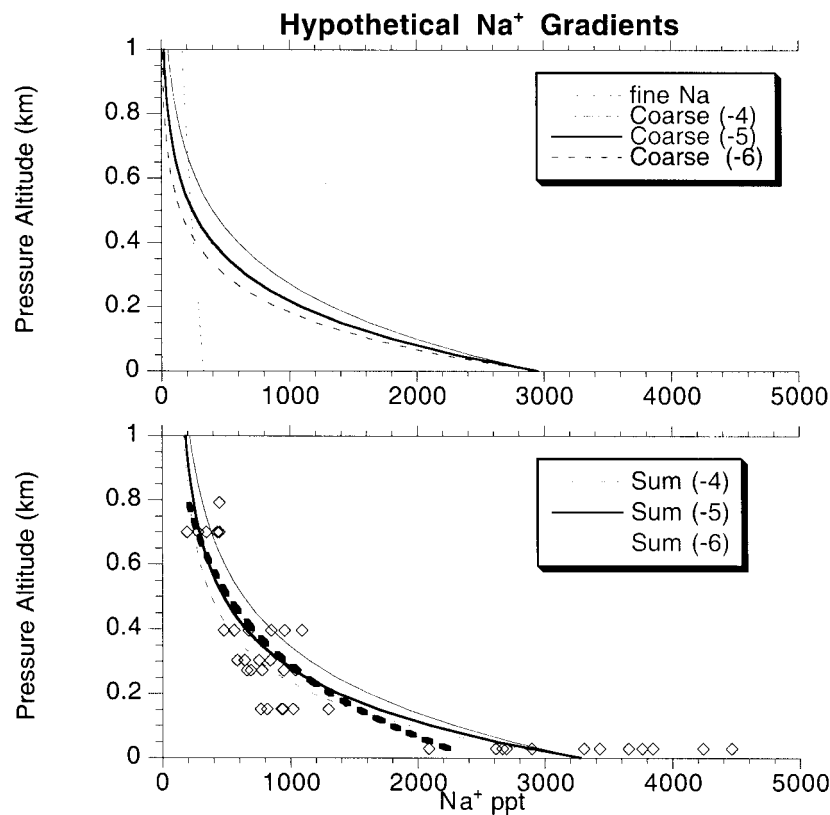


**Figure 10.** Hypothetical  $\text{Na}^+$  gradients, all of the form  $\text{MR} = \text{MR}_0 e^{(R \cdot \text{Alt})}$  where  $R$  is assumed to be  $-0.7$  for fine ( $<2$  micron) sea-salt aerosols and arbitrarily set at  $-4$ ,  $-5$ , and  $-6$  for coarser particles.  $\text{MR}_0$  is selected to be the mean measured at the tower (3300 ppt) but is partitioned 10% to the fine fraction and 90% to the coarse. In the lower panel the labeled curves are the sum of the fine and each of the hypothetical coarse profiles, with the heavy dashed curve the best fit exponential from Figure 9. Diamonds in the lower panel are the measurements from Figure 9.

dominantly distributed to supermicron particles does not help this argument very much, but they are all consistent with this view. At the 30 m level on the tower,  $\text{MS}^-$  was distributed nearly evenly between submicron and 1–6 micron particles (Table 2). The exponential fit to  $\text{MS}^-$  mixing ratios on 21–22 March UT (Figure 11, top panel) yields estimated surface mixing ratios that are just 1% higher than the mean measured at the tower. In this case, the scatter at all altitudes is considerable with a much lower  $R$  value than found for the sea-salt species. Part of this may be due to analytical uncertainty at low mixing ratios, but we suspect that the fact that  $\text{MS}^-$  must be formed from DMS and then attach to aerosol particles, rather than being emitted directly from the ocean, is also contributing to the variability. Nitrate in the tower impactor samples was dominantly ( $>97\%$ ) supermicron, with 15% of its mass associated with particles  $>6$  microns (Table 2). The vertical distribution of  $\text{NO}_3^-$  is poorly described by an exponential decrease with height (Figure 11, bottom panel), though the mean at the tower was just 2% higher than the surface mixing ratio estimated from the curve fit. The theory predicting exponential decay with height was developed for particles generated mechanically (by wave breaking and bubble bursting) at the surface, and then lost by dry

deposition back to the surface. The P-3  $\text{HNO}_3$  data set reveals an opposite trend to particulate  $\text{NO}_3^-$ , decreasing nearly 30 ppt between the free troposphere and boundary layer (Figure 12). The increase in particle  $\text{NO}_3^-$  as the ocean surface is approached is more likely due to increasing uptake of  $\text{HNO}_3$  as available particle surface area increases, rather than oceanic emission. In any case, if our airborne aerosol system was not efficiently passing supermicron aerosols we would expect to see offsets between the mixing ratios of  $\text{MS}^-$  and  $\text{NO}_3^-$  measured on the tower and those collected higher up from the P-3. No such offsets are apparent (Figure 11).

[25] Total  $\text{SO}_4^{2-}$  provides our final example of an aerosol-associated species dominated by the supermicron fraction (70%  $>1$  micron, 30%  $>5$  microns (Table 2)). Unlike the sea-salt species,  $\text{SO}_4^{2-}$  has a significant (30%) submicron fraction. The vertical distribution of total  $\text{SO}_4^{2-}$  on 21–22 March UT is reasonably well described by an exponential decrease with height (Figure 13, top panel). Notably, the rate of decrease is 1/3 that of the completely sea-salt derived species (Figure 9), consistent with a larger fraction of mass being associated with smaller particles. Further, the estimated surface mixing ratio is identical to the mean measured at the tower. This latter point is no doubt fortuitous,

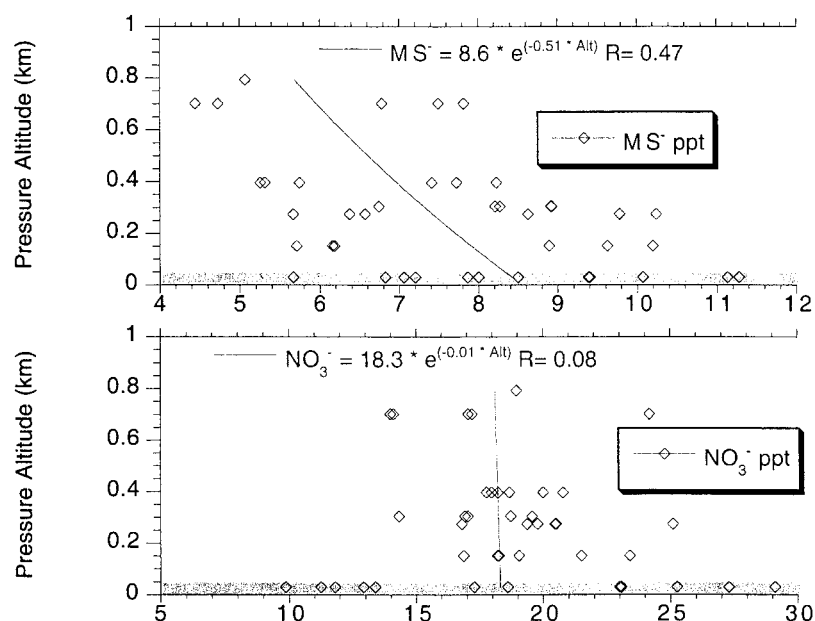


Figure 11. As in Figure 9 but for  $\text{MS}^-$  and  $\text{NO}_3^-$ .

given the range of mixing ratios in the tower samples, but overall the total  $\text{SO}_4^{2-}$  vertical profile gives no indication that the airborne samples are seriously biased against supermicron particles.

[26] Given the evidence that our P-3 sampling system must be passing a high percentage of particles with diameters up to 6 microns (or even larger) we assume that accumulation mode aerosols are sampled essentially quantitatively. Non-sea-salt  $\text{SO}_4^{2-}$  and  $\text{NH}_4^+$  were both found predominantly in the submicron mode at the tower (Table 2) hence are the best tracers of fine particles in our data set. The vertical distributions of these species in the P-3 samples below 1 km can be reasonably described by exponential decreases with height, at rates a bit slower than found for total  $\text{SO}_4^{2-}$  (Figure 12, lower panels). However, nearly all of

the  $\text{NH}_4^+$  mixing ratios measured from the P-3 below 0.6 km were greater than the mean measured at 30 m from the tower. In the case of nss  $\text{SO}_4^{2-}$  all P-3 samples below 0.6 km exceeded the maximum mixing ratio measured at the tower, with half the P-3 samples above 0.6 km greater than the tower mean. As a result, estimated surface mixing ratios from the fits to the P-3 nss  $\text{SO}_4^{2-}$  and  $\text{NH}_4^+$  data greatly overestimate the means at the tower and attempting to fit exponential curves to the combined data sets is pointless.

[27] The discrepancies between the tower and P-3 measurements of ions largely associated with accumulation mode particles are puzzling, and potentially negate all of the foregoing comparisons between the two data sets. One explanation could be that the air masses reaching Christmas Island on 22 March (local time) were so dissimilar to the

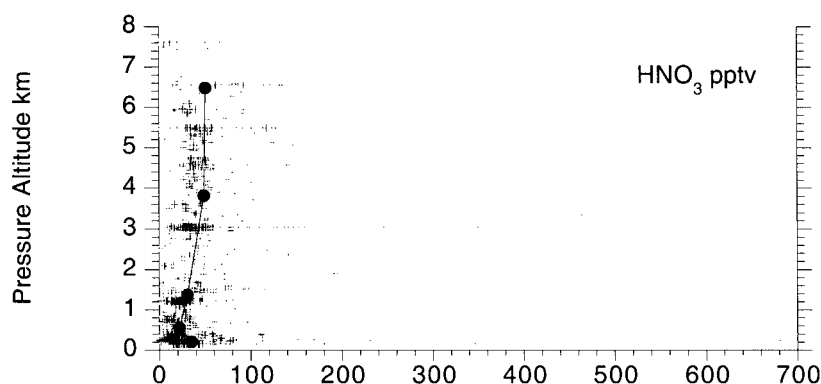
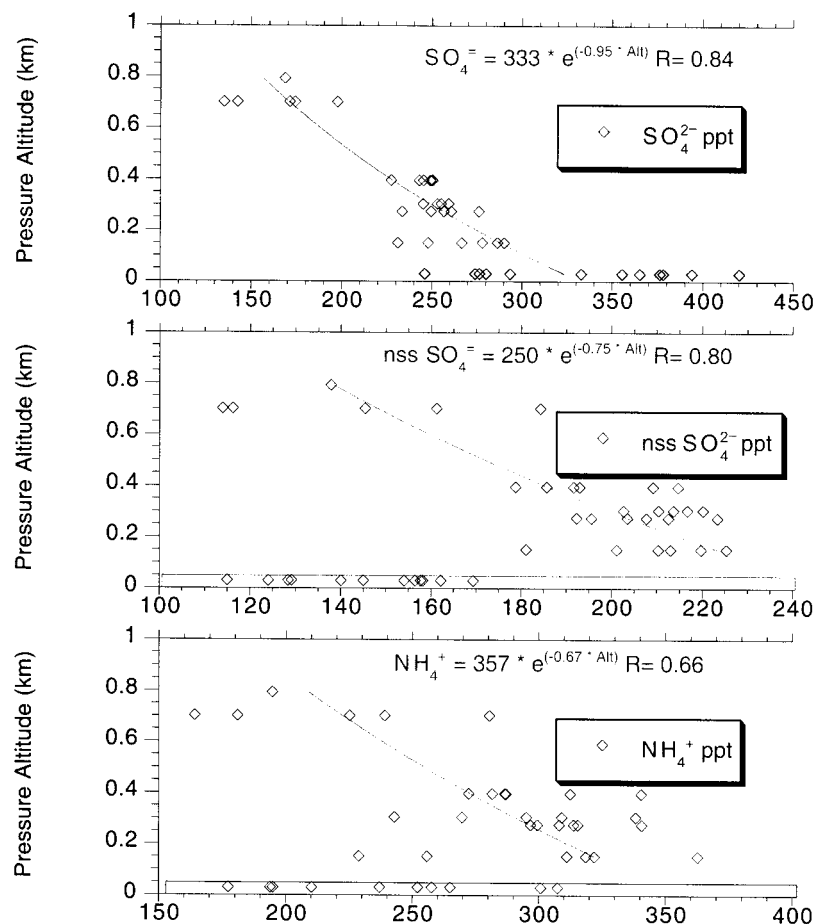


Figure 12. Nitric acid measured from the P-3 during PEM-Tropics B Flights 5–12 in the vicinity of Christmas Island. The large dots are plotted at the mean mixing ratios in the same altitude bins used for Figures 1 and 2. No  $\text{HNO}_3$  measurements were made on Christmas Island.



**Figure 13.** As in Figure 9 but for total  $\text{SO}_4^{2-}$ , nss  $\text{SO}_4^{2-}$  and  $\text{NH}_4^+$ . For the latter two species the measurements at the tower are shown in the box along the ordinate, but are not included in the curve fit.

equatorial air mass sampled by the P-3 10–20 h later that we really can not compare the two. However, mixing ratios of DMS in whole air samples collected into canisters (and analyzed as described by I. J. Simpson et al. (Aircraft measurements of dimethyl sulfide (DMS) using a whole air sampling technique, submitted to *Journal of Atmospheric Chemistry*, 2000)) on the P-3 and the Christmas Island tower display a smooth exponential decrease with height (Figure 14), suggesting that the sea to air flux of DMS was similar in the vicinity of Christmas Island and in the P-3 sampling region. (See *Atlas et al.* [2002] for details of tower sampling for trace gases and discussion of the results for many additional compounds.) Observations of  $\text{CH}_3\text{I}$  from the tower and the P-3 likewise suggest relatively homogeneous conditions in the study area during the two days of interest (Figure 14). On the other hand, bromoform and methyl nitrate, two additional trace gases with dominant oceanic sources in the central Pacific [*Atlas et al.*, 1993, 1997; *Blake et al.*, 1999, this issue], resembled nss  $\text{SO}_4^{2-}$  and  $\text{NH}_4^+$  in that mixing ratios were considerably higher at P-3 sampling altitudes than at the tower (Figure 14). These observations indicate that any assertion of spatial homogeneity must be species dependent, but it does not appear that large differences in the source strength of DMS between the equatorial P-3 sampling region and Christmas Island can be

the dominant contributor to the discrepancy in nss  $\text{SO}_4^{2-}$  mixing ratios measured from the two platforms.

[28] It is also possible that much of the nss  $\text{SO}_4^{2-}$  and  $\text{NH}_4^+$  in the upper part of the marine boundary layer that we could sample from the P-3 is not derived from the local surface ocean. Long-range transport of anthropogenic emissions from Asia, and perhaps north America, within the free troposphere, and subsequent downward mixing could constitute a significant nonmarine source of both  $\text{SO}_4^{2-}$  and  $\text{NH}_4^+$  in the marine boundary layer around Christmas Island. Two lines of evidence cause us to discount this possibility for the central equatorial Pacific during the PEM-Tropics B investigation. First, the mixing ratios of both species were generally much higher in the marine boundary layer than in the overlying free troposphere (Figures 1 and 2), making it difficult to envision the latter acting as a source for the former. Second, a suite of hydrocarbon and halocarbon tracers of industrial emissions were measured in whole air samples collected on the P-3 and DC-8 during PEM-Tropics B [*Blake et al.*, 2001]. These data clearly show intrusions of polluted northern hemisphere air into the southern hemisphere. These intrusions were largely restricted to altitudes below 2 km and to the western Pacific. In the equatorial region sampled on P-3 flights from Christmas Island, enhancements of the reactive hydro-



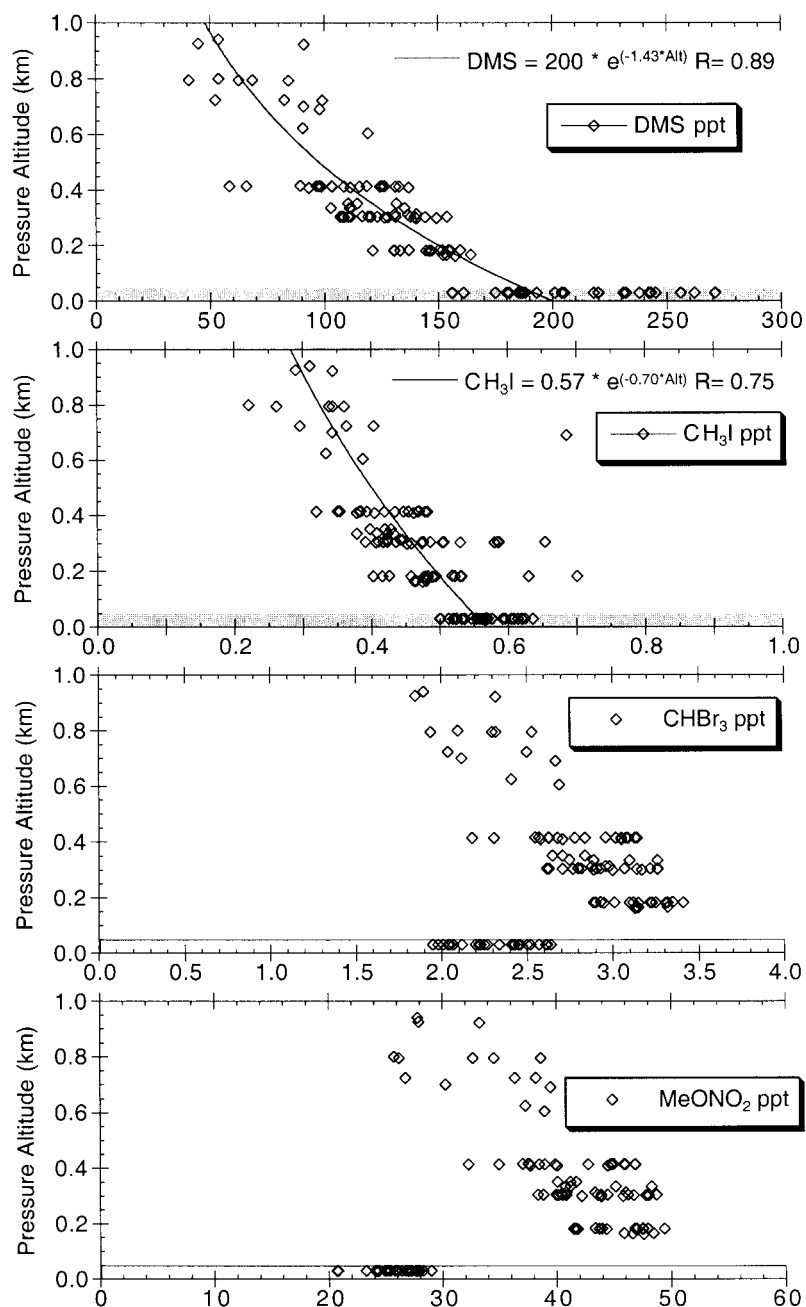


**Figure 14.** As in Figure 9 but for several trace gases emitted from the ocean: dimethyl sulfide, methyl iodide, bromoform, and methyl nitrate. Because the tower measurements are so much lower than those from the P-3, no curve fits are shown for bromoform and methyl nitrate, though both clearly decrease rapidly with altitude in the P-3 data set.

carbon tracers were subtle at best, suggesting that intrusions of northern hemispheric air were less frequent or weaker than was the case further west. *Blake et al.* [2001] point out that, in general, hydrocarbon/CO ratios in equatorial regions sampled during PEM-Tropics B were low, suggesting that the air masses had significantly aged since last receiving anthropogenic emissions. It therefore seems likely that the dominant source of nss  $\text{SO}_4^{2-}$  and  $\text{NH}_4^+$  in the marine boundary layer around Christmas Island must be the tropical Pacific ocean.

[29] Recognizing that nss  $\text{SO}_4^{2-}$  is a derived value, based on measurements of  $\text{SO}_4^{2-}$  and a sea-salt tracer ( $\text{Mg}^{2+}$  in our case), we have considered whether the calculation introduces the discrepancy between the P-3 and tower data sets. Poor passing efficiency of larger particles through the P-3 system would lead to underestimation of sea-salt mixing ratios, hence might lead to overestimation of nss  $\text{SO}_4^{2-}$ . However, large particle  $\text{SO}_4^{2-}$  is considered to be part of the coarse sea-salt particles, so any inlet losses should impact  $\text{SO}_4^{2-}$  and the sea-salt tracer to similar extents. In any case,

we should see more direct evidence of this problem in the distributions of sea-salt species (Figure 9) and the other species with significant supermicron fractions (Figures 11 and 13, upper panel). Furthermore, this explanation does not apply to  $\text{NH}_4^+$  at all, yet the  $\text{NH}_4^+$  mixing ratios from the P-3 are as much “too high” as are those of nss  $\text{SO}_4^{2-}$  (Figure 13, lower panels). Like  $\text{MS}^-$ ,  $\text{NH}_4^+$  and nss  $\text{SO}_4^{2-}$  in the marine boundary layer are not primary aerosols, but result from gas to particle conversion processes. In this regard, one might expect  $\text{MS}^-$  and nss  $\text{SO}_4^{2-}$  distributions to be somewhat linked, with  $\text{NH}_4^+$  perhaps divergent, since we believe that  $\text{NH}_3$  is directly emitted from the ocean while the two S species are products of DMS oxidation and their gaseous precursors may have vertical distributions that differ from  $\text{NH}_3$ . On the other hand, the well established tendency for  $\text{MS}^-$  to have a much more significant supermicron fraction than nss  $\text{SO}_4^{2-}$  (Table 2) [see also Quinn *et al.*, 1993; Huebert *et al.*, 1993, 1996; Andreae *et al.*, 1995], though not well understood, suggests that the fate of soluble gaseous compounds like  $\text{H}_2\text{SO}_4$ , MSA and  $\text{NH}_3$  in the marine boundary layer must be controlled by multiple factors in addition to vertical distribution.

[30] Overall, the comparisons between aerosol-associated soluble ions collected from the P-3 and the Christmas Island tower suggest that inlet concerns should have little impact on P-3 data for nss  $\text{SO}_4^{2-}$ ,  $\text{NH}_4^+$  and  $\text{MS}^-$ . The sea-salt comparisons suggest, but do not prove, that our airborne system efficiently collects particles up to nearly 9 microns, such that the P-3 data on particulate  $\text{NO}_3^-$  are also likely to be substantially correct. Of course, these comparisons also highlight the need for much further work on gas to particle conversion in the marine boundary layer.

## 5. Conclusions

[31] Sampling the ambient aerosol from aircraft without significant inlet-related fractionation is a difficult task, and also one that is hard to assess. Our comparisons between bulk aerosol collected from the P-3 and at 30 m above sea level illustrate the problems one encounters in assessing inlet passing efficiency, but also indicate that the system we flew on the P-3 must be sampling a high percentage of particles with diameters up to 6 microns, and possibly as large as 10 microns. Because the P-3 aerosol probe is modeled on the probe we fly on the Dryden DC-8, we assume that the DC-8 probe performs similarly. Clearly, we must continue seeking opportunities to more fully characterize the transmission efficiency of our airborne aerosol sampling probes. The apparent transmission efficiency of the P-3 probe increases our confidence in aerosol data from the DC-8 that we have published and publicly archived for GTE missions since PEM West A, as well as SUCCESS and SONEX. In particular, we suspect that it is very unlikely that inlet losses of free tropospheric  $\text{SO}_4^{2-}$  could be anywhere close to 50%.

[32] Our observation of higher mixing ratios of dominantly accumulation mode nss  $\text{SO}_4^{2-}$  and  $\text{NH}_4^+$  between 150 and 600 m, compared to 30 m, are not fully understood. The smooth decrease of DMS with altitude in the combined data set indicates that the jump in nss  $\text{SO}_4^{2-}$  between the tower and the lowest P-3 sampling altitude can not be

readily attributed to spatial variability (in source strength or removal by scavenging). It may be that nss  $\text{SO}_4^{2-}$  and  $\text{NH}_4^+$  mixing ratios are depressed just above the ocean by condensation onto larger particles that are quickly removed by dry deposition. Clearly, this point requires considerable further work including additional measurements to confirm our observations and model studies that include realistic size-resolved aerosol populations in and above the marine boundary layer along with gas phase S and  $\text{NH}_3$  fluxes and chemistry.

[33] **Acknowledgments.** We thank the flight and ground crews of the Wallops Island P-3 for their excellent support throughout PEM-Tropics B. Discussions with the entire PEM-Tropics B science team inspired and improved this manuscript. This research was supported by the NASA Global Tropospheric Chemistry Program.

## References

- Andreae, M. O., W. Elbert, and S. J. de Mora, Biogenic sulfur emissions and aerosols over the tropical South Atlantic, 3, Atmospheric dimethylsulfide, aerosols and cloud condensation nuclei, *J. Geophys. Res.*, **100**, 11,335–11,356, 1995.
- Atlas, E., W. Pollock, J. Greenberg, L. Heidt, and A. M. Thompson, Alkyl nitrates, nonmethane hydrocarbons, and halocarbon gases over the equatorial Pacific Ocean during SAGA 3, *J. Geophys. Res.*, **98**, 16,933–16,949, 1993.
- Atlas, E., F. Flocke, S. Schauffler, V. Stroud, D. Blake, and F. S. Rowland, Evidence for marine sources of atmospheric alkyl nitrates: Measurements over the tropical Pacific Ocean during PEM-Tropics, *Eos Trans. AGU*, **78**(46), 1997.
- Atlas, E., et al., Trace gas measurements in the marine boundary layer at Christmas Island during PEM-Tropics B, *J. Geophys. Res.*, submitted manuscript, 2002.
- Bandy, A. R., D. C. Thornton, B. W. Blomquist, S. Chen, T. P. Wade, J. C. Ianni, G. M. Mitchell, and W. Nadler, Chemistry of dimethyl sulfide in the equatorial Pacific atmosphere, *Geophys. Res. Lett.*, **23**, 741–744, 1996.
- Bates, T. S., A. D. Clarke, V. N. Kapustin, J. E. Johnson, and R. J. Charlson, Oceanic dimethylsulfide and marine aerosol: Difficulties associated with assessing their covariance, *Global Biogeochem. Cycles*, **3**, 299–304, 1989.
- Bates, T. S., J. A. Calhoun, and P. K. Quinn, Variations in the methane-sulfonate to sulfate molar ratio in submicrometer marine aerosol particles over the south Pacific ocean, *J. Geophys. Res.*, **97**, 9859–9865, 1992.
- Baumgardner D., B. Huebert, and C. Wilson, Meeting review: Airborne aerosol inlet workshop, *NCAR Tech. Note TN-362+1A*, 288 pp., Natl. Cent. for Atmos. Res., Boulder, Colo., 1991.
- Blake, N. J., et al., Aircraft measurements of the latitudinal, vertical, and seasonal variations of NMHCs, methyl nitrate, methyl halides, and DMS during the First Aerosol Characterization Experiment (ACE 1), *J. Geophys. Res.*, **104**, 21,803–21,817, 1999.
- Blake, N. J., D. R. Blake, E. Atlas, F. Flocke, and F. S. Rowland, Latitudinal, vertical and seasonal variations of  $\text{C}_1$ – $\text{C}_4$  alkyl nitrates in the troposphere over the Pacific Ocean during PEM Tropics A and B: Oceanic and continental sources, *J. Geophys. Res.*, this issue.
- Blake, N. J., et al., Large scale latitudinal and vertical distribution of NMHCs and selected halocarbons in the troposphere over the Pacific Ocean during the March–April 1999 Pacific Exploratory Expedition (PEM-Tropics B), *J. Geophys. Res.*, **106**(D23), 32,627–32,644, 2001.
- Blanchard, D. C., and A. H. Woodcock, The production, concentration and vertical distribution of the sea-salt aerosol, in *Aerosols: Anthropogenic and Natural, Sources and Transport*, Ann. N. Y. Acad. Sci., vol. 338, edited by T. J. Kneip and P. J. Lioy, pp. 330–347, New York Academy of Sciences, New York, 1980.
- Chin, M., D. L. Savoie, B. J. Huebert, A. R. Bandy, D. C. Thornton, T. S. Bates, P. K. Quinn, E. S. Saltzman, and W. J. De Bruyn, Atmospheric sulfur cycle simulated in the global model GOCART: Comparison with field observation and regional budgets, *J. Geophys. Res.*, **105**, 24,689–24,712, 2000.
- Clarke, A. D., and J. N. Porter, Pacific marine aerosol, 2, Equatorial gradients in chlorophyll, ammonium and excess sulfate during SAGA 3, *J. Geophys. Res.*, **98**, 16,997–17,010, 1993.
- Davis, D., PEM-Tropics (B) Science Team, The Pacific Exploratory Mission-Tropics B (PEM-Tropics B): Objectives, execution and overview of results for the P-3B component, *J. Geophys. Res.*, submitted manuscript, 2002a.
- Davis, D., et al., A case study of the marine sulfur budget based on P-3

- airborne observations recorded during PEM-Tropics B, *J. Geophys. Res.*, submitted manuscript, 2002b.
- Dibb, J. E., R. W. Talbot, K. I. Klemm, G. L. Gregory, H. B. Singh, J. D. Bradshaw, and S. T. Sandholm, Asian influence over the western North Pacific during the fall season: Inferences from lead-210, soluble ionic species, and ozone, *J. Geophys. Res.*, *101*, 1779–1792, 1996.
- Dibb, J. E., R. W. Talbot, B. L. Lefter, E. Scheuer, G. L. Gregory, E. V. Browell, J. D. Bradshaw, S. T. Sandholm, and H. B. Singh, Distributions of beryllium-7, lead-210, and soluble aerosol-associated ionic species over the western Pacific: PEM-West B February–March, 1994, *J. Geophys. Res.*, *102*, 28,287–28,302, 1997.
- Dibb, J. E., R. W. Talbot, and M. B. Loomis, Tropospheric sulfate distribution during SUCCESS: Contributions from jet exhaust and surface sources, *Geophys. Res. Lett.*, *25*, 1375–1378, 1998.
- Dibb, J. E., R. W. Talbot, E. M. Scheuer, D. R. Blake, N. J. Blake, G. L. Gregory, G. W. Sachse, and D. C. Thornton, Aerosol chemical composition and distribution during the Pacific Exploratory Mission, Tropics, *J. Geophys. Res.*, *104*, 5785–5800, 1999.
- Dibb, J. E., R. W. Talbot, and E. M. Scheuer, Composition and distribution of aerosols over the North Atlantic during the Subsonic Assessment Ozone and Nitrogen Oxide Experiment (SONEX), *J. Geophys. Res.*, *105*, 3709–3717, 2000.
- Giannakopoulos, C., M. P. Chipperfield, K. S. Law, and J. A. Pyle, Validation and intercomparison of wet and dry deposition schemes using  $^{210}\text{Pb}$  in a global three-dimensional off-line chemical transport model, *J. Geophys. Res.*, *104*, 23,761–23,784, 1999.
- Giannakopoulos, C., M. P. Chipperfield, K. S. Law, P. H. Plantevin, J. A. Pyle, and D. E. Shallcross, A three-dimensional modeling study of the correlations of  $^{210}\text{Pb}$  with  $\text{HNO}_3$  and peroxyacetylnitrate (PAN) at remote oceanic sites, *J. Geophys. Res.*, *105*, 1947–1956, 2000.
- Guelle, W., Y. J. Balkanski, J. E. Dibb, M. Schulz, and F. Dulac, Wet deposition in a global size-dependent aerosol transport model, 2, Influence of the scavenging scheme on  $^{210}\text{Pb}$  vertical profiles, surface concentrations, and deposition, *J. Geophys. Res.*, *103*, 28,875–28,891, 1998.
- Huebert, B. J., G. Lee, and W. L. Warren, Airborne aerosol inlet passing efficiency measurement, *J. Geophys. Res.*, *95*, 16,369–16,381, 1990.
- Huebert, B. J., S. Howell, P. Laj, J. E. Johnson, T. S. Bates, P. K. Quinn, V. Yegorov, A. D. Clarke, and J. N. Porter, Observations of the atmospheric sulfur cycle on SAGA 3, *J. Geophys. Res.*, *98*, 16,985–16,995, 1993.
- Huebert, B. J., D. J. Wylie, L. Zhuang, and J. A. Heath, Production and loss of methanesulfonate and non-sea salt sulfate in the equatorial Pacific marine boundary layer, *Geophys. Res. Lett.*, *23*, 737–740, 1996.
- Jacob, D. J., et al., The Pacific Exploratory Mission-Tropics B (PEM-Tropics B): Objectives, execution and overview of results for the DC-8 component, *J. Geophys. Res.*, special section on PEM Tropics B, in press.
- Neele, F. P., G. de Leeuw, A. M. J. van Eijk, E. Vignati, M. K. Hill, and M. H. Smith, Aerosol production in the surf zone and effects on IR extinction, *NATO RTO Meet. Proc.*, *1*, 24-1–24-11, 1998.
- Nowack, J. B., et al., DMSO: A new source of marine sulfur, *J. Geophys. Res.*, submitted manuscript, 2002.
- Oncley, S., N. Blake, I. Simpson, D. Blake, and L. Thornhill, Trace gas fluxes obtained from canister samples using cospectral similarity, *J. Geophys. Res.*, submitted manuscript, 2002.
- Porter, J. N., A. D. Clarke, G. Ferry, and R. F. Pueschel, Aircraft studies of size-dependent aerosol sampling through inlets, *J. Geophys. Res.*, *97*, 3815–3824, 1992.
- Quinn, P. K., T. S. Bates, J. E. Johnson, D. S. Covert, and R. J. Charlson, Interactions between the sulfur and reduced nitrogen cycles over the central Pacific ocean, *J. Geophys. Res.*, *95*, 16,405–16,416, 1990.
- Quinn, P. K., D. S. Covert, T. S. Bates, V. N. Kapustin, D. C. Ramsey-Bell, and L. M. McInnes, Dimethylsulfide/cloud condensation nuclei/climate system: Relevant size-resolved measurements of the chemical and physical properties of atmospheric aerosol particles, *J. Geophys. Res.*, *98*, 10,411–10,427, 1993.
- Raper, J. L., M. M. Kleb, D. J. Jacob, D. D. Davis, R. E. Newell, H. E. Fuelberg, R. J. Bendura, J. M. Hoell, and R. J. McNeal, Pacific Exploratory Mission in the Tropical Pacific: PEM-Tropics B, March–April 1999, *J. Geophys. Res.*, *106*(D23), 32,401–32,425, 2001.
- Savoie, D. L., J. M. Prospero, R. Arimoto, and R. A. Duce, Non-sea-salt sulfate and methanesulfonate at American Samoa, *J. Geophys. Res.*, *99*, 3587–3596, 1994.
- Xiao, H., G. R. Carmichael, J. Durchenwald, D. Thornton, and A. Bandy, Long-range transport of Sox and dust in East Asia during the PEM B experiment, *J. Geophys. Res.*, *102*, 28,589–28,612, 1997.

E. Atlas, ACD, NCAR, Boulder, CO, USA.

D. R. Blake and N. J. Blake, Chemistry Department, University of California-Irvine, Irvine, CO, USA.

J. E. Dibb, R. W. Talbot, G. Seid, C. Jordan, and E. Scheuer, Institute for the Study of Earth, Oceans, and Space, University of New Hampshire, Durham, NH 03824, USA. (jack.dibb@unh.edu)